

Spontaneous optical pattern formation in a large array of optoelectronic feedback circuits

Mikhail A. Vorontsov, Gary W. Carhart, and Rensheng Dou

*Army Research Laboratory, Information Science and Technology Directorate, AMSRL-IS-C,
2800 Powdermill Road, Adelphi, Maryland 20783*

Received April 23, 1999; revised manuscript received August 31, 1999

Strong nonlinear optical effects and optical pattern-forming systems can be designed with the optical system architectures introduced here on the basis of large-scale arrays of optoelectronic feedback circuits. Experiments were performed with a liquid-crystal television panel as a large-scale array of phase modulators and a CCD camera as a photoarray. By synthesizing various nonlinearities and using controllable spatial coupling, we obtained a variety of transversal optical patterns, localized states, waves, and chaotic regimes. © 2000 Optical Society of America [S0740-3224(00)00602-0]
OCIS codes: 190.0190, 200.0200, 250.0150, 190.4420.

1. INTRODUCTION

Progress in nonlinear optics, and particularly in the area of transversal nonlinear optical effects, is very much dependent on the development of new nonlinear materials. Despite impressive advances recently achieved in this field, the long-held dream of having optical nonlinearities that are both strong and fast has yet to be realized. We still must choose between materials that have either a strong but slow or a weak but fast nonlinear response. With a cubic optical nonlinearity, this means that in the classical dependence $n = n_0 + n_2 I$ linking the medium refractive index n to the incident light intensity I , a higher value of the nonlinear parameter n_2 can be achieved primarily at the expense of having a longer nonlinear response time τ_{nl} .¹

Researchers in the field of spatiotemporal dynamics are perhaps the most anxious for strong nonlinearities—large n_2 at any expense—as the most intriguing and remarkable transversal effects such as spontaneously emerging optical patterns, solitary structures, waves, and chaotic regimes occur in wide-aperture optical systems.² In addition, most transversal phenomena are extremely sensitive to the quality (uniformity) of the incident-beam intensity and phase profile. In most cases the required laser beam quality can be achieved only with an additional increase in the power level.

These buzz words—large n_2 at any expense—are not completely true because formation of optical patterns, localized states, waves, and other transversal optical instabilities typically occur at transition times on the order of several hundred τ_{nl} . In practice, this bounds the nonlinear response time, since a transition process should be completed at least during a time psychologically comfortable for the researcher. If we consider information–image processing—perhaps the major promise in nonlinear dynamics—the response time should be decreased by at least two orders of magnitude. There are no nonlinear materials that can provide both strong ($n_2 > 0.1 \text{ cm}^2/\text{mW}$) and relatively fast ($\tau_{nl} < 10^{-3} \text{ s}$)

nonlinear responses, but there are some tricks that can be used for synthesizing strong optical nonlinearity effects without the direct use of natural microscopic nonlinear materials.

In this paper we show that strong optical nonlinearity effects and optical systems for transversal pattern formation studies (pattern-forming systems) can be designed with large-scale arrays of optoelectronic feedback circuits. A related approach was first implemented in incoherent pictorial feedback systems (a television camera looking into its own monitor that was connected with the camera through a nonlinear digital video processing system).³ Here, the feedback video processing system is used to control a coherent wave spatial phase distribution. In Section 2 we describe a generic hybrid optoelectronic pattern-forming system that contains an electrically addressed large-scale (high-resolution) array of phase modulators coupled with an array of photodetectors through an optical and electronic feedback loop. Electronic signal–image processing in the system's feedback loop allows us to synthesize not only cubic (Kerr)-type nonlinearity (practically as strong as we need) but also a variety of more sophisticated nonlinearities (binary, unimodal, bimodal, etc.) that are difficult or even impossible to obtain with natural microscopic nonlinear materials.

In the experiments performed with a liquid-crystal television (LCTV) panel as a large-scale array of phase modulators and a CCD camera as a photoarray, we observed a dazzling variety of static and dynamic optical patterns, waves, localized states, and chaotic regimes. In Section 3 we present an overview (taxonomy) of the observed transverse spatiotemporal instabilities (definitely not yet completed) obtained with different nonlinearity types.

The approach presented here can be used not only as a convenient vehicle for the study of self-organization phenomena but also as a practical tool for the generation of laser beams with controllable spatiotemporal intensity and phase distributions. In Section 3 we demonstrate a self-organized controllable array of localized states (spa-

tial solitons) obtained with the system introduced here based on large-scale arrays of optoelectronic feedback circuits.

Problems relating to the design and applications of artificial nonlinearities with new advanced technologies such as micro-electro-mechanical systems (MEMS mirrors) and analog parallel very large-scale integration (VLSI) microelectronic systems are discussed in the Concluding Remarks.

2. HYBRID OPTOELECTRONIC PATTERN-FORMING SYSTEM

A. Nonlinearity Design Aspects

Strong optical nonlinearities for transversal optical pattern formation can be synthesized using optically addressed spatial light modulators (OASLM's) based on various electro-optical effects.⁴ In a typical phase OASLM, the output wave spatial phase modulation is dependent on the light intensity illuminating the OASLM's photoconductive layer (controlling light).⁴ In an optical two-dimensional (2D) feedback-system configuration the output wave is also used as a controlling light. In this case the dependence of wave-front modulation on beam intensity is similar to that of a microscopic media with cubic nonlinear response. Thus the phase OASLM in a 2D feedback configuration can be considered as a thin nonlinear slice modeling a cubic optical nonlinearity (Kerr slice). This approach was first implemented in pattern-forming systems that use a liquid-crystal light-valve (LCLV) phase modulator.⁵ The equivalent nonlinear parameter n_2 for a LCLV feedback system can exceed $0.1 \text{ cm}^2/\text{mW}$ with a typical time response of $\tau_{nl} \sim 0.1 \text{ s}$. At present LCLV feedback systems are widely used to study a variety of transversal nonlinear effects.⁶

The use of optically addressed phase spatial light modulators as the nonlinear element in pattern-forming systems has several limitations. Physical processes that occur in these types of optoelectronic devices are complex, and the commonly used Kerr-type models describing OASLM dynamics are quite simplified.⁴ This complicates understanding and interpretation of the transversal effects most often observed in experiments. Furthermore, optically addressed phase modulators have a relatively large time response ($\tau_{nl} \sim 0.1 \text{ s}$) and typically suffer from a notable level of parasitic phase modulation (phase noise) related to nonuniformities in the photoconductive layer.⁴ Perhaps the major drawback of both OASLM-based and purely optical pattern-forming systems is the lack of flexibility for implementation of the different nonlinearity types typically required for specific nonlinear dynamics applications.⁷ With nonlinear materials the type of nonlinearity is a built-in form of a specific light-matter interaction mechanism, and in OASLM devices the type of nonlinearity depends on the electrooptical effect used.

B. Large-Scale Array of Optoelectronic Feedback Circuits: System Architecture and Models

Recent advances in microelectronics, in particular in the areas of analog parallel VLSI computational systems,⁸ large-scale (high-resolution) arrays of MEMS mirrors,⁹

and liquid-crystal (LC)-on-silicon phase modulators,¹⁰ have made practical implementation of novel optical pattern-forming system architectures with large-scale arrays of optoelectronic feedback circuits possible.⁷ The general concept of a hybrid optoelectronic pattern-forming system is shown in Fig. 1. A coherent input optical wave with complex amplitude $A_0(\mathbf{r})$ ($\mathbf{r} = \{x, y\}$ is a vector in the transverse plane) is reflected from an array of microactuators (micromirrors or LC cells). The number of microactuators N in an array may exceed $10^5 - 10^6$.¹¹ Microactuators introduce a controllable phase modulation $u(\mathbf{r}, t)$. The depth of phase modulation is dependent on the controlling signal $v(\mathbf{r}, t)$ formed by an electronic (analog or digital) feedback signal processing system: $u(\mathbf{r}, t) = U[v(\mathbf{r}, t)]$, where U is an operator describing dynamics of an individual actuator. For the sake of simplicity, consider here a linear dependence: $u(\mathbf{r}, t) = \gamma v(\mathbf{r}, t)$, where γ is a constant.¹²

Reflected from the microactuator array, the phase-modulated wave $A(\mathbf{r}, t) = A_0(\mathbf{r})\exp[i u(\mathbf{r}, t)]$ enters the feedback loop that contains both optical and electronic signal processing systems as shown in Fig. 1. The optical signal processing system's output intensity $I_d(\mathbf{r}, t)$ is registered by a photoarray interfaced with an electronic feedback signal processing system. We assume that the microactuator and photoarrays are optically matched; that is, they have the same size and pixel geometry.

The entire system spatiotemporal dynamics depend on the type of signal processing realized in the system feedback loop. Consider the following model that can be implemented with specially designed parallel image processing hardware— analog VLSI or digital signal processing systems:

$$\tau \frac{\partial v(\mathbf{r}, t)}{\partial t} + v = \mathbf{d}\nabla_{\perp}^2 v + K w_{\text{FB}}(\mathbf{r}, t),$$

$$\left(\nabla_{\perp}^2 = \frac{\partial^2}{\partial x^2} + \frac{\partial^2}{\partial y^2} \right), \quad (1)$$

$$w_{\text{FB}}(\mathbf{r}, t) = \int \Phi[I_d(\mathbf{r}', t)] h(\mathbf{r} - \mathbf{r}') d^2\mathbf{r}', \quad (2)$$

$$I_d(\mathbf{r}, t) = O[A(\mathbf{r}, t)],$$

$$A(\mathbf{r}, t) = A_0(\mathbf{r})\exp[i\gamma v(\mathbf{r}, t)]. \quad (3)$$

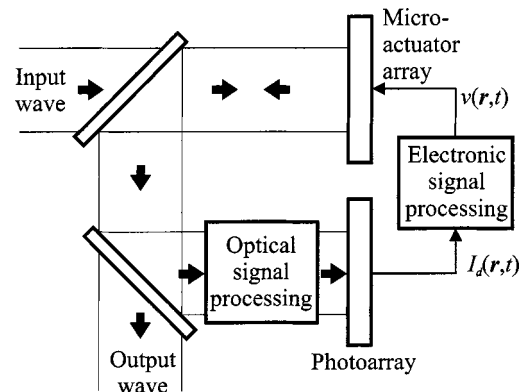


Fig. 1. Schematic for a pattern-forming system based on a large-scale array of optoelectronic feedback circuits.

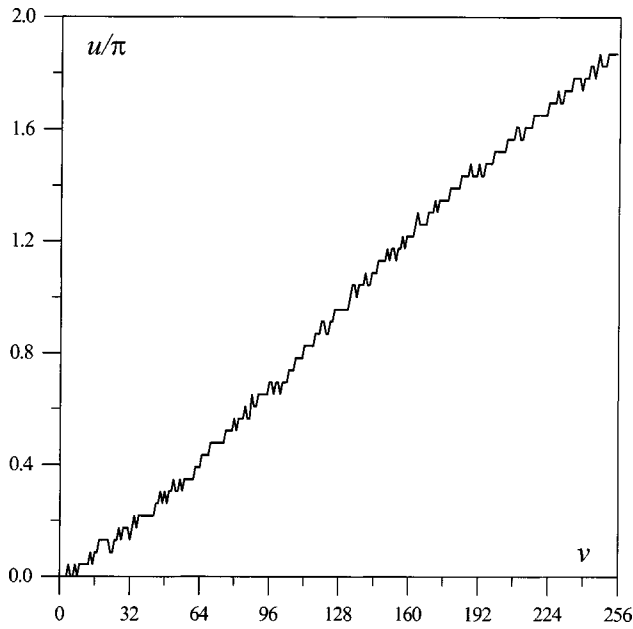


Fig. 3. Characteristic phase modulation of the LCTV panel.

For solution of the nonlinear diffusion equation (7), we used the alternating directions method.¹⁷ To keep phase modulation in the operational range of the LCTV panel (0–255 gray levels), the aperture minimum value $\min_{x,y} \nu^{(n+1)}(\mathbf{r})$ was subtracted from the obtained signal $\nu^{(n+1)}(\mathbf{r})$. The convolution integral in Eq. (8) was calculated with the spectral representation of Eq. (8): $W_{\text{FB}}^{(n)}(\mathbf{q}) = F\{\Phi[I_d^{(n)}]\}H(\mathbf{q})$, where \mathbf{q} is spatial frequency, $W_{\text{FB}}^{(n)}(\mathbf{q})$ and $H(\mathbf{q})$ are the spatial spectral amplitudes for $w_{\text{FB}}^{(n)}(\mathbf{r})$ and $h(\mathbf{r})$, and $F\{\}$ is the Fourier transform operator. The transfer function $H(\mathbf{q})$ used in our calculations corresponded to a low-pass spatial filter with cutoff frequency q_{cut} : $H(\mathbf{q}) = \exp[-|\mathbf{q}|/q_{\text{cut}}]^8$ (super-Gaussian filter). Along with digital filtering, we also used a low-pass optical Fourier filter. In this case,

$$I_d(\mathbf{r}, t) = \left| \int A(\mathbf{r}', z=L, t) h_{\text{opt}}(\mathbf{r} - \mathbf{r}') d^2\mathbf{r}' \right|^2, \quad (9)$$

where $h_{\text{opt}}(\mathbf{r})$ is the Fourier transform of the optical low-pass filter. Optical feedback processing included free-space propagation [Eq. (6)] and Fourier filtering [Eq. (9)].

3. OPTICAL PATTERN FORMATION IN THE OPTOELECTRONIC FEEDBACK SYSTEM

A. Kerr-Type Nonlinearity: Hexagonal Patterns

The hexagonal patterns emerging in a purely optical Kerr-slice-feedback-mirror system provide an excellent proof-of-concept test for the optoelectronic pattern-forming system. The following discrete-time approximation for the continuous model [Eqs. (4)–(6)] was used in experiments:

$$\begin{aligned} \nu^{(n+1)}(\mathbf{r}) = & (1 - \alpha)\nu^{(n)}(\mathbf{r}) \\ & + \Delta I_{\perp}^{(n)}\nu^{(n)}(\mathbf{r}) + KI_d^{(n)}(\mathbf{r}). \end{aligned} \quad (10)$$

For the case of spatial filtering we also used the signal processing model [Eqs. (7) and (8)] with linear dependence $\Phi[I_d^{(n)}] = \gamma I_d^{(n)}$ as presented by line 1 in Fig. 4.

In the absence of both digital and optical spatial filtering the system was unstable if the feedback gain coefficient K exceeded a threshold value K_{th} . When $|K|$ was increased above K_{th} , we observed a spontaneous transition from a spatially uniform intensity distribution toward hexagonal patterns and then further to disordered patterns similar to what was reported in Kerr-slice-feedback-mirror systems with purely optical nonlinear media, or in LCLV-based feedback systems.¹⁸ The hexagonal transversal optical patterns—diffractive intensity and controlling patterns [phase images $u(\mathbf{r})$]—are shown in Fig. 5. The bright spots in the hexagonal pattern in Fig. 5(b) cover approximately four pixels of the LCTV panel. Dependent on the sign of the feedback gain coefficient K , we observed hexagonal patterns typical for both self-defocusing and self-focusing cases. Spatial nonuniformity of the LCTV transmittance (~ 10 – 15% across the aperture) as well as a residual (noncompensated) mismatch between image sizes in the LCTV panel and CCD array planes resulted in dislocations of the hexagonal pattern in Fig. 5. Stable hexagonal patterns were obtained only for relatively small values of the update coefficient $\alpha < 0.2$ in Eq. (10). For $\alpha > 0.2$, approximation of the continuous-time equation (4) by the discrete model [Eq. (10)] is not stable, which results in the disintegration of hexagons and the appearance of traveling wave-type instabilities.

The pattern formation process appeared to be rather sensitive to the alignment of optical components with small misalignment, leading to motion of the entire hexagonal pattern. We also examined dynamics of the optoelectronic Kerr-slice-feedback-mirror system without diffusion ($d = 0$). For this case local spatial coupling was introduced by use of digital or optical low-pass spatial filters. Stable hexagonal patterns similar to those shown

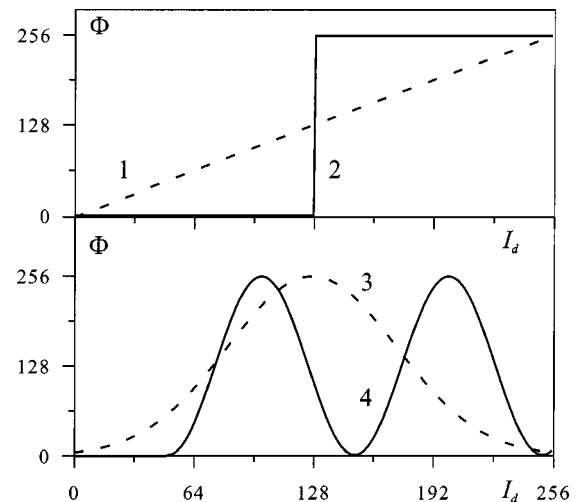


Fig. 4. Nonlinearity types used in the experiments: (1) linear dependence between intensity and phase corresponding to Kerr-type nonlinearity; (2) binary nonlinearity; (3) unimodal (Gaussian) nonlinearity; and (4) bimodal (sine-type) nonlinear function. Both the input diffractive intensity and the transformed signal $\Phi(I_d)$ are measured in video signal gray levels.

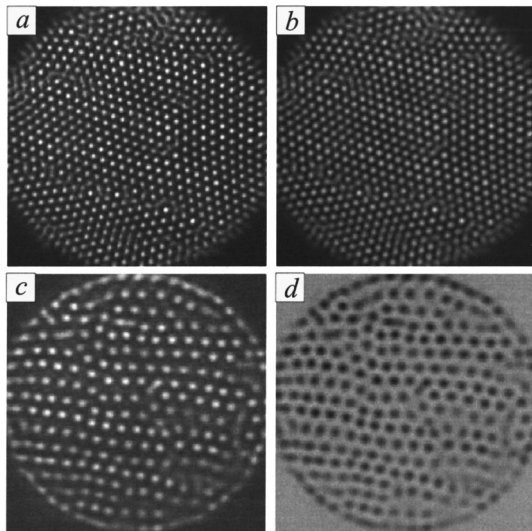


Fig. 5. Hexagonal patterns in optoelectronic Kerr-slice-feedback-mirror system corresponding to (a), (b) self-defocusing nonlinearity ($n_{\text{FB}} < 0$) and (c), (d) self-focusing nonlinearity ($n_{\text{FB}} > 0$); (a), (c) diffractive beam intensity patterns $I_d(\mathbf{r})$; and (b), (d) corresponding controlling images $\nu(\mathbf{r})$ sent to the LCTV panel (phase images). The laser beam diameter in the plane of the LCTV equals 20 mm. System parameters are $L = 8$ mm, $|K| \geq 1.2 K_{\text{th}}$, $d = 0.0001$, $\alpha = 0.1$.

in Fig. 5 were observed for the spatial filter cutoff frequency $q_{\text{cut}} > q_1$, where q_1 is a critical spatial filter radius determined from linear stability analysis: $q_1 = \pi\sqrt{2}(\lambda L)^{-1/2}$ for self-focusing and $q_1 = \pi\sqrt{3}(\lambda L)^{-1/2}$ for self-defocusing.¹⁶ For q_{cut} slightly less than q_1 , we also observed square-type periodical patterns.

B. Kerr-Type Nonlinearity with Field Rotation: Optical Quasi-Crystals

Consider pattern formation in the hybrid optoelectronic system having azimuthal field rotation in the optical feedback. Field rotation in the 2D feedback loop represents an example of long-range spatial coupling. Long-range spatial coupling in transversal nonlinear optics was first introduced in the LCLV-based nonlinear interferometer with 2D feedback.^{5,19} More recently, 2D feedback field rotation was combined with diffraction (LCLV-based diffractive feedback system with field rotation).²⁰ These types of systems have displayed a vast range of static and dynamics spatiotemporal instabilities (rotary waves, quasi crystals, pattern competition, chaotic regimes).^{20,21}

In the system shown in Fig. 2, azimuthal field rotation was implemented by rotation of the CCD camera at a fixed angle Δ around the system's optical axes. The intensity registered by the CCD camera can be represented in a cylindrical coordinate system as $I_d^{(n)}(\mathbf{r}_\Delta)$, where $\mathbf{r}_\Delta = \{\rho, \theta + \Delta\}$ is a vector in the plane of the camera. In the system with field rotation the electronic feedback signal processing equation (10) reads as

$$\nu^{(n+1)}(\mathbf{r}) = (1 - \alpha)\nu^{(n)}(\mathbf{r}) + d\Delta_\perp^{(n)}\nu^{(n)}(\mathbf{r}) + KI_d^{(n)}(\mathbf{r}_\Delta). \quad (11)$$

To control the feedback signal spatial spectrum content, we used an optical low-pass spatial filter. The size of the filter's diaphragm was adjusted to block all except the

lowest instability band. By varying the system parameters (feedback gain coefficient, rotation angle, and filtering diaphragm size), we obtained a variety of self-organized nonlinear patterns. In the experiments we also observed pattern competition, periodic and chaotic alternation, and chaotic spatiotemporal regimes. An example of pattern alternation obtained in the system with field rotation for self-focusing Kerr-type nonlinearity is shown in Fig. 6. The pattern alternation consisted of a repeating sequence of quasi-stationary patterns. Pattern alternation has been analyzed both in nonlinear systems with macroscopic nonlinearities (photorefractive ring oscillator²²) and in LCLV systems.²³ In the experiments with the optoelectronic feedback system, we observed alternating sequences that contained from three to ten different quasi-stable patterns—only three patterns are presented in Fig. 6. Note that similar dynamics were also obtained that used electronic feedback with diffusion instead of optical low-pass filtering.

C. Binary Nonlinearity: Localized States

It has been recently demonstrated that several nonlinear optical systems are capable of generating a set of intensity peaks in a laser beam cross section known as diffractive autosolitons, spatial solitons, or localized states—

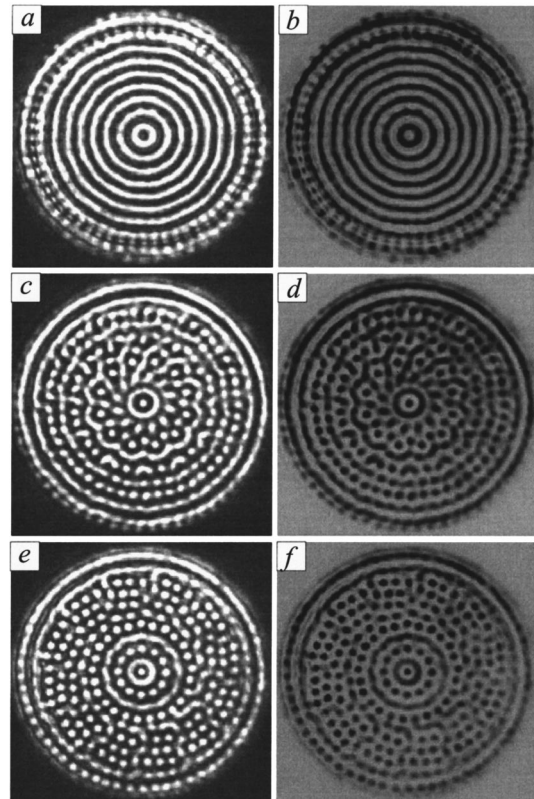


Fig. 6. Chaotic alternation between different transversal quasi-stable patterns observed in the experiment with feedback field rotation. The diffractive intensity patterns (a), (c), and (e) and the corresponding phase images (b), (d), and (f) are shown in their order of consecutive appearance: (a), (b) $n = 400$; (c), (d) $n = 640$; (e), (f) $n = 720$. The system parameters are $\Delta = 30$ deg., $\alpha = 0.2$, $d = 0$, $K = 0.1$, $L = 8$ mm, $I_0 = 97$. The input intensity I_0 here and below corresponds to an aperture-averaged value measured in the CCD camera in video signal gray levels.

other terms are also used.²⁴ To designate these intensity peaks and avoid potential terminological problems, we use localized states (LS's) as the most general term. The simplest optical system having LS's as a steady-state pattern consists of a binary-phase slice and a feedback mirror. Binary-type (stepwise) nonlinearity has been introduced as a model of microscopic nonlinearities with strong saturation when transition between unsaturated and saturated levels occurs within a narrow interval of intensity change for the refractive index in a nonlinear medium.²⁵ Theoretical analysis and numerical simulations of the binary-phase slice and feedback-mirror model predicted the existence of LS's whose arrangement depends on input beam spatial intensity and phase modulation. These LS properties have the potential to be used for nonlinear image processing.²⁵

Consider implementation of the binary-slice–feedback-mirror model with the hybrid optoelectronic feedback system shown in Fig. 2. The optical processing included only free-space propagation over the distance L . Electronic signal processing was based on Eqs. (7) and (8) with stepwise function Φ shown by curve 2 in Fig. 4.

LS's were experimentally observed for a negative feedback gain coefficient K in the presence of a low-pass spatial filter having the relatively narrow bandwidth $0.4q_1 < q_{\text{cut}} < 0.85q_1$. Typical patterns for LS's are shown in Figs. 7(a) and 7(b). The LS's have formed clusters as seen in Fig. 7(a). The number of LS's in a cluster was dependent on either the input intensity or the feedback gain coefficient. The LS position depends on local modulation of the input beam phase or intensity or both. The LS's in Figs. 7(a) and 7(b) are grouped along the inhomogeneities of the input beam intensity resulting from parasitic intensity modulation introduced by the LCTV panel.

D. Unimodal Nonlinearity: Web-Pattern and Black Holes

Flexibility in nonlinearity choice is one of the major benefits of the optoelectronic pattern-forming system. Artificial nonlinearities synthesized in the optoelectronic feedback loop may dramatically enrich the palette of nonlinear spatiotemporal phenomena. A simple example of artificial nonlinearity is provided by the unimodal function Φ shown by curve 3 in Fig. 4.

The system with unimodal nonlinearity displayed spectacularly rich dynamics. For a positive feedback gain coefficient K and electronic spatial filtering, we observed LS's as shown in Figs. 7(c) and 7(d). In contrast, with the case of binary nonlinearity the LS's did not form clusters but merged under collision. The LS position can be controlled by the introduction of a small phase modulation (seed phase pattern) as discussed in Ref. 26. In the experiment the hexagonal-type phase seed-image shown in Fig. 8(b) was introduced as an additional driving signal applied to the LCTV panel. This seed phase-image resulted in the formation of a self-organized array of LS's in Fig. 8(a). Note that the technique can be applied to create controllable and self-adaptive diffractive optics elements in place of a conventional microlens array.²⁷

The case of negative K is particularly interesting. When the input beam intensity was increased, we observed a consecutive transition from the loosely organized

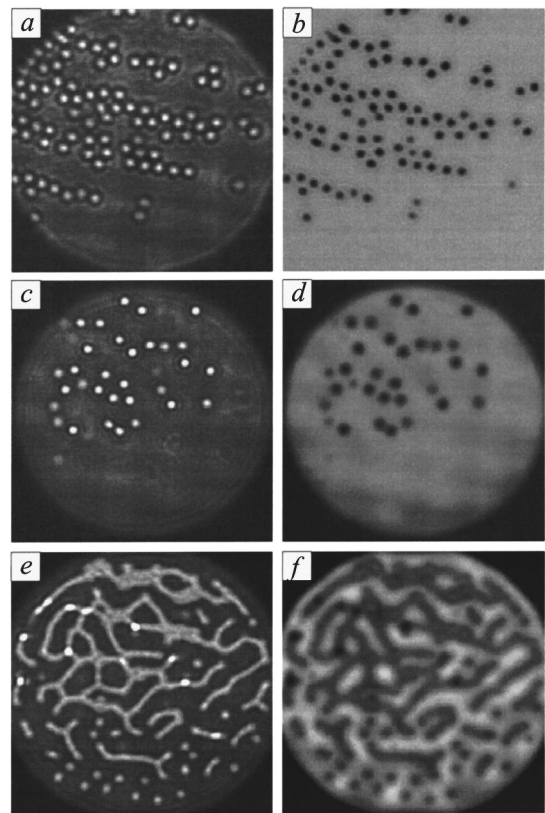


Fig. 7. Intensity pattern of localized states (left-hand column) and phase patterns (right-hand column) obtained in the pattern-forming system with the nonlinearity types shown in Fig. 4: (a), (b) binary; (c), (d) unimodal (Gaussian); and (e), (f) bimodal (sine-type). Spatial filter cutoff frequencies are $q_{\text{cut}} = 0.7q_1$ for binary, $q_{\text{cut}} = 0.4q_1$ for unimodal, and $q_{\text{cut}} = 0.5q_1$ for bimodal nonlinearities. Here and below $q_1 = \pi\sqrt{3}(\lambda L)^{-1/2}$. The input intensities are (a), (b) $I_0 = 82$; (c), (d) $I_0 = 111$; and (e), (f) $I_0 = 120$. System parameters are $d = 0$, $\alpha = 0.2$, $K = 0.1$, $L = 12$ mm.

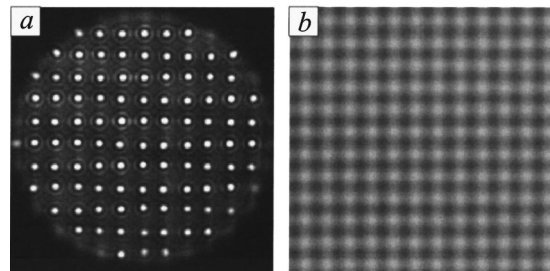


Fig. 8. Self-organized array of localized states (a) in the system with unimodal nonlinearity in the presence of the external phase modulation (b) [seed pattern]. The amplitude of phase modulation in the seed pattern comprises 8% of the LCTV panel dynamical range. The system parameters are the same as in Figs. 7(c) and 7(d).

pattern in Figs. 9(a) and 9(b) to the web pattern in Figs. 9(c) and 9(d) and further to a set of black holes in Figs. 9(e) and 9(f). The formation of the web pattern occurred through a cascade of web-cell division bifurcation. The size of the cells corresponding to a stationary-state web pattern was dependent on the electronic spatial filter cutoff frequency. Patterns similar to those shown in Fig. 9 were observed in the system with electronically intro-

duced diffusion and with the use of a purely optical low-pass filter.

E. Bimodal Nonlinearity: Black-Eye Array, Localized States, Chaotic Regimes

Bimodal nonlinearity as shown by a segment of the sine function in Fig. 4 (curve 4) represents one more example of an artificially created phase-intensity dependence. The bimodal (N - or S -shape) nonlinearity is one of the cornerstones in modern nonequilibrium system theory and synergetics.²⁸ The dynamical model [Eqs. (1) and (2)] with bimodal-type nonlinear function represents an example of nonlinear diffusion or a Fisher–Kolmogorov–Petrovskii–Piskunov (FKPP)-type equation, widely used in nonlinear dynamical systems in optics, chemistry, and biology.²⁹ In the optoelectronic pattern-forming system the FKPP process is used in conjunction with wave diffraction and can be described by a coupled nonlinear diffusion–diffraction-type model.³⁰

In the experiments we used both optical and electronic spatial filtering that was applied instead of diffusion. In most cases we obtained similar dynamics as in the case of pure diffusive spatial coupling. For a positive feedback gain coefficient and relatively narrow low-bandpass filtering, we observed extraordinary LD's as shown in Figs. 7(e) and 7(f). Intensity peaks in Figs. 7(e) and 7(f) have

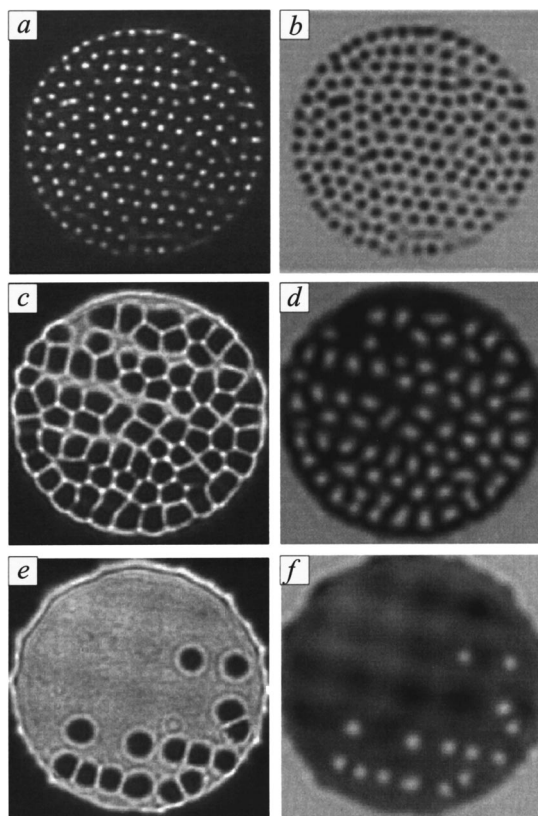


Fig. 9. Pattern formation in the system with unimodal nonlinearity. Intensity (left-hand column) and phase (right-hand column) patterns for different input beam intensity I_0 values measured in the CCD camera in video signal gray levels: (a), (b) disordered bright spots, $I_0 = 55$; (c), (d) web pattern, $I_0 = 97$; and (e), (f) black holes, $I_0 = 140$. The system parameters are $q_{\text{cut}} = 0.6q_1$, $L = 12$ mm, $d = 0$, $\alpha = 0.2$, and $K = -0.1$.

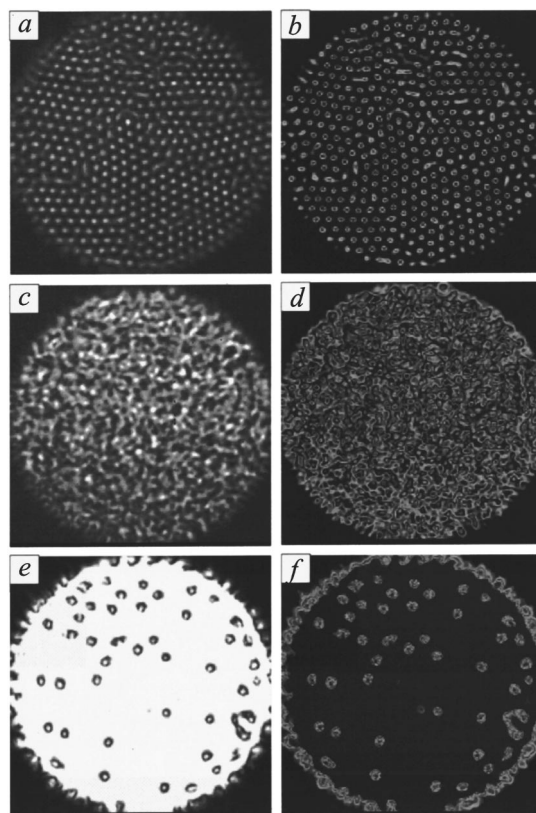


Fig. 10. Pattern formation in the system with bimodal nonlinearity. Intensity (left-hand column) and phase (right-hand column) patterns for different input beam intensity I_0 values measured in the CCD camera in video signal gray levels: (a), (b) black-eye array, $I_0 = 70$; (c), (d) chaotic pattern, $I_0 = 134$; and (e), (f) black-eye localized states, $I_0 = 200$. The system parameters are $q_{\text{cut}} = 4.0q_1$, $L = 12$ mm, $d = 0$, $\alpha = 0.2$, and $K = -0.1$.

two distinct intensity levels: warm and hot spots. The hot spots always belonged to lines, and the warm spots existed alone.

The most remarkable spatiotemporal phenomena were observed in the system with a negative feedback gain coefficient and with a wide-band low-pass spatial filter. When the input intensity level (or the feedback gain coefficient) was increased, the spatially uniform intensity and phase pattern became unstable, giving rise to the black-eye phase pattern shown in Fig. 10(a). A further increase in intensity leads to the development of a chaotic intensity and phase modulation as seen in Figs. 10(c) and 10(d). The chaotic regime exists in a relatively narrow intensity window, and as intensity was further increased, black eyes returned in the form of LS's [Figs. 10(e) and 10(f)].

4. CONCLUDING REMARKS

The system introduced here with optoelectronically (artificially) designed optical nonlinearity can be considered as a hybrid optoelectronic computer that combines two signal processing paradigms: continuously distributed optical processing and discrete electronic (analog or digital) computations. Both the input and output signals are

real optical fields interfaced with a discrete signal processing system through high-resolution arrays of phase actuators and sensors.

With the recent development of systems having large arrays of milli- and microscale actuators and sensors (smart and adaptive structures), problems related to the control of such structures become important. Control is based on local information received by the sensor array. Through a large array of feedback circuits, this information is used to compute the actuator's control signals. Spatiotemporal instabilities that can potentially arise in such systems are an important issue. Design, optimization, and stability analysis of parallel feedback-control architectures for smart structures are emerging in a number of areas: optics, acoustics, biomedicine, hydrodynamic, etc. A good example is the control of fluid-structure interaction based on large arrays of MEMS actuators and sensors.³¹

In comparison with other fields, in optics we actually have the most advanced tools for prototyping, modeling, and analyzing the dynamics of structures composed of large arrays of actuators and sensors interfaced through feedback circuits. In the proof-of-concept experiments described here, we used commercially available building blocks—the LCTV panel, CCD camera, and PC computer—hardware that is definitely not optimal. The low operational speed (~ 1.2 s per iteration)—a major drawback of this system—resulted from the mismatch between the size and number of pixels of the LCTV panel and CCD camera. This mismatch required time-consuming digital scaling of the registered intensity patterns. With customer-designed phase actuators and sensors arrays, this problem can be overcome.

With currently available large-scale arrays of MEMS mirrors optically coupled with photoarray and analog parallel VLSI systems for feedback signal processing, the characteristic system response time can be less than 10^{-3} s with a spatial resolution of the order of 512×512 or even 1024×1024 elements. This could potentially provide small, efficient hybrid optoelectronic computational architectures for modeling and studying a variety of complex nonlinear spatiotemporal phenomena. These systems can also be used for the generation of complex optical field structures, parallel image processing, and in adaptive optics applications.

ACKNOWLEDGMENTS

We thank J. C. Ricklin for technical and editorial comments. Work was performed at the Army Research Laboratory's Intelligent Optics Lab in Adelphi, Maryland.

The corresponding author, Mikhail A. Vorontsov, can be reached at the address on the title page or by telephone at 301-394-0214, by fax at 301-394-0225, or by e-mail at vorontsov@iol.arl.mil.

REFERENCES AND NOTES

- H. M. Gibbs, *Optical Bistability—Controlling Light with Light* (Academic, Orlando, Fla., 1985); I. R. Shen, *The Principles of Nonlinear Optics* (Wiley, New York, 1984).
- J. V. Moloney and A. C. Newell, *Nonlinear Optics* (Addison-Wesley, Redwood City, Calif., 1991); L. A. Lugiato, M. Brambilla, and A. Gatti, "Optical pattern formation," *Adv. At. Mol. Opt. Phys.* **40**, 229–306 (1998); M. A. Vorontsov and W. B. Miller, eds., *Self-Organization in Optical Systems and Applications in Information Technology* (Springer, Berlin, 1995); C. O. Weiss, "Spatio-temporal structures. Part II," *Phys. Rep.* **219**, 311–328 (1992).
- G. Hausler and M. Simon, "Generation of space and time picture oscillations by active incoherent feedback," *Opt. Acta* **25**, 327–336 (1978); J. P. Crutchfield, "Space-time dynamics in video-feedback," *Physica D* **10**, 229–338 (1984); G. Hausler, G. Seckmeyer, and T. Weiss, "Chaos and cooperation in nonlinear pictorial feedback systems," *Appl. Opt.* **25**, 4656–4663 (1986).
- U. Efron, ed., *Spatial Light Modulator Technology: Materials, Devices, and Applications* (Marcel Dekker, New York, 1995); V. G. Chigrinov, *Liquid Crystal Devices: Physics and Applications* (Artech House, Norwood, Mass., 1999).
- M. A. Vorontsov, Yu. D. Dumarevsky, D. V. Pruidze, and V. I. Shmalhauzen, "Autowave processes in optical feedback systems," *Izv. Akad. Nauk SSSR, Ser. Fiz.* **52**, 374–376 (1988); S. A. Akhmanov, M. A. Vorontsov, and V. Yu. Ivanov, "Large-scale transverse nonlinear interactions in laser beams; new types of nonlinear waves; onset of optical turbulence," *JETP Lett.* **47**, 611–614 (1988).
- S. A. Akhmanov, M. A. Vorontsov, V. Yu. Ivanov, A. V. Larichev, and N. I. Zheleznykh, "Controlling transverse-wave interactions in nonlinear optics: generation and interaction of spatiotemporal structures," *J. Opt. Soc. Am. B* **9**, 78–90 (1992); R. Neubecker, G. L. Oppo, B. Thuring, and T. Tschudi, "Pattern formation in a liquid-crystal light valve with feedback, including polarization, saturation, and internal threshold effects," *Phys. Rev. A* **52**, 791–808 (1995); P. L. Ramazza, E. Pampaloni, S. Residori, and F. T. Arecchi, "Optical pattern formation in a Kerr-like medium with feedback," *Physica D* **96**, 259–271 (1996).
- M. A. Vorontsov, "Information processing with nonlinear optical two-dimensional feedback systems," *J. Opt. B: Quantum Semiclass. Opt.* **1**, R1–R10 (1999).
- C. A. Mead, "Neuromorphic electronic systems," *Proc. IEEE* **78**, 1629–1640 (1990); R. P. Lippmann and D. S. Touretzky, eds., *Neural Information Processing Systems*, (Morgan Kaufmann, San Mateo, Calif., 1995), Vol. 3.
- M. C. Wu, "Micromachining for optical and opto-electronic systems," *Proc. IEEE* **85**, 1833–1997 (1997); G. V. Vdovin and P. M. Sarro, "Flexible mirror micromachined in silicon," *Appl. Opt.* **34**, 2968–2972 (1995).
- S. Serati, G. Sharp, R. Serati, D. McKnight, and J. Stookley, "128 × 128 analog liquid crystal spatial light modulator," in *Optical Pattern Recognition VI*, D. P. Casasent and T.-H. Chao, eds., *Proc. SPIE* **2490**, 55–63 (1995); <http://www.bnnonlinear.com>.
- Currently developed arrays of turntable micromirrors as well as arrays of LC-on-silicon phase modulators may have 512×512 actuators with actuator (pixel) size less than $100 \mu\text{m}$ for MEMS and $15 \mu\text{m}$ for LC devices.
- High-spatial resolution of both the micromirror and the photoarray allows the use of continuous-form mathematical models.
- L. A. Lugiato and M. S. El Nashie, eds., Special issue on nonlinear optical structures, patterns, and chaos, *Chaos, Solitons, and Fractals* **4**, 1251–1844 (1994).
- A. G. Andreou and K. A. Boahen, "Translinear circuits in subthreshold MOS," *Analog Integr. Circuits and Signal Process.* **9**, 141–153 (1996).
- G. Giusfredy, J. F. Valley, R. Pon, G. Khitrova, and H. M. Gibbs, "Optical instabilities in sodium vapor," *J. Opt. Soc. Am. B* **5**, 1181–1192 (1988).
- W. J. Firth, "Spatial instabilities in a Kerr medium with a single feedback mirror," *J. Mod. Opt.* **37**, 151–155 (1990); G. P. D'Alessandro and W. J. Firth, "Hexagon spatial patterns for a Kerr slice with a feedback mirror," *Phys. Rev. A* **46**, 537–548 (1992); M. A. Vorontsov and W. Firth, "Pattern formation and competition in nonlinear optical systems

- with two-dimensional feedback," *Phys. Rev. A* **49**, 2891–2903 (1994).
17. W. F. Ames, *Numerical Methods for Partial Differential Equations* (Academic, San Diego, Calif., 1992).
 18. R. Neubecker, B. Thuring, and T. Tschudi, "Formation and characterization of hexagonal patterns in a single feedback experiment," in a special issue on nonlinear optical structures, patterns, and chaos, *Chaos, Solitons, and Fractals* **4**, L. A. Lugiato and M. S. El Nashie eds., 1307–1322 (1994); M. Tamburrini and E. Ciaramella, "Hexagonal beam filamentation in a liquid crystal film with single feedback mirror," 1355–1367.
 19. H. Adachihara and H. Faid, "Two-dimensional nonlinear-interferometer pattern analysis and decay of spirals," *J. Opt. Soc. Am. B* **10**, 1242–1253 (1993); N. I. Zheleznykh, M. Le Berre, F. Ressayre, and A. Tallet, "Rotating spiral waves in a nonlinear optical system with spatial interaction," in *Chaos, Solitons and Fractals*, L. A. Lugiato and M. S. El Nashie, eds. (Pergamon, New York, 1994).
 20. M. A. Vorontsov, "'Akhseals' as a new class of spatio-temporal light field instabilities," *Quantum Electron.* **23**, 269–271 (1993); M. A. Vorontsov, N. G. Iroshnikov, and R. Abernathy, "Diffractive patterns in a nonlinear optical 2D-feedback system with field rotation," in *Chaos, Solitons and Fractals*, L. A. Lugiato and M. S. El Nashie, eds. (Pergamon, New York, 1994).
 21. E. Pampaloni, P. L. Ramazza, S. Residori, and F. T. Arecchi, "Two-dimensional crystals and quasicrystals in nonlinear optics," *Phys. Rev. Lett.* **74**, 258–261 (1995); B. Y. Rubinstein and L. M. Pismen, "Resonant two-dimensional patterns in optical cavities with rotated beam," *Phys. Rev. A* **56**, 4264–4272 (1997).
 22. F. T. Arecchi, S. Boccaletti, G. Giacomelli, P. L. Ramazza, and S. Residori, "Pattern and vortex dynamics in photorefractive oscillators," in *Self-Organization in Optical Systems and Applications in Information Technology*, M. A. Vorontsov and W. B. Miller, eds. (Springer, New York, 1995).
 23. F. T. Arecchi, "Optical morphogenesis: pattern formation and control in nonlinear optics," *II Nuovo Cimento A* **107**, 1111–1121 (1994).
 24. N. N. Rosanov and G. V. Khodova, "Diffractive autosolitons in nonlinear interferometers," *J. Opt. Soc. Am. B* **7**, 1057–1065 (1990); D. V. McLaughlin, J. V. Moloney, and A. C. Newel, "Solitary waves as fixed points of infinite-dimensional maps in an optical bistable ring resonator," *Phys. Rev. Lett.* **51**, 75–78 (1983); G. S. McDonald and W. J. Firth, "Spatial solitary-wave optical memory," *J. Opt. Soc. Am. B* **7**, 1328–1335 (1990); Y. S. Kivshar and Xiaoping Yang, "Dynamics of dark solitons," in *Chaos, Solitons and Fractals*, L. A. Lugiato and M. S. El Nashie, eds. (Pergamon, New York, 1994), p. 1745.
 25. M. A. Vorontsov and B. A. Samson, "Nonlinear dynamics in an optical system with controlled 2D-feedback: black-eye patterns and related phenomena," *Phys. Rev. A* **57**, 3040–3049 (1998).
 26. R. Martin, A. J. Scroggie, G. L. Oppo, and W. J. Firth, "Stabilization and tracking of unstable patterns by Fourier space techniques," *Phys. Rev. Lett.* **77**, 4007–4012 (1996); W. J. Firth and A. J. Scroggie, "Optical bullet holes: robust controllable localized states of a nonlinear cavity," *Phys. Rev. Lett.* **76**, 1623–1626 (1996).
 27. J. N. Mait, "Diffractive beauty," *Opt. Photon. News* **9**, 21–25 (1998).
 28. H. Haken, *Synergetics, an Introduction* (Springer-Verlag, Berlin, 1997); G. Nicolis, *Introduction to Nonlinear Science* (Cambridge U. Press, Cambridge, UK, 1995).
 29. Y. Kuramoto, *Chemical Oscillations, Waves and Turbulence* (Springer-Verlag, Berlin, 1984); G. H. Gunaratne, Q. Ouyang, and H. L. Swinney, "Pattern formation in the presence of symmetries," *Phys. Rev. E* **50**, 2802–2820 (1994).
 30. E. V. Degtiarev and V. G. Watagin, "Stability analysis of a two-component nonlinear system," *Opt. Commun.* **124**, 309–313 (1996).
 31. C.-M. Ho and Y.-C. Tai, "Micro-electro-mechanical-systems and fluid flows," *Annu. Rev. Fluid Mech.* **30**, 579–612 (1998).